

**Design of a Flapping Mechanism for
Reproducing the Motions at the Base of a Dragonfly Wing**

by

Teresa Liu

Submitted to the Department of Mechanical Engineering
in Partial Fulfillment of the Requirements for the Degree of

Bachelor of Science
at the
Massachusetts Institute of Technology

June 2007

© 2007 Teresa Liu. All Rights Reserved

The author hereby grants to MIT permission to reproduce and to distribute publicly
paper and electronic copies of this thesis document in whole or in part
in any medium now known or hereafter created.

Signature of Author

Department of Mechanical Engineering
May 11, 2007

Certified by

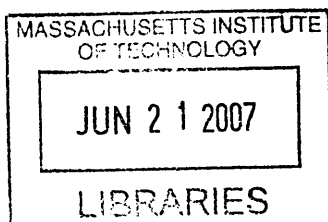
/
Lynette A. Jones
Principal Research Scientist, MIT BioInstrumentation Lab
Thesis Co-supervisor

Certified by

James Louis Tangorra
~~Postdoctoral Associate, MIT BioInstrumentation Lab~~
Thesis Co-supervisor

Accepted by

John H. Lienhard V
Professor of Mechanical Engineering
Chairman, Undergraduate Thesis Committee



ARCHIVES

Design of a Flapping Mechanism for
Reproducing the Motions at the Base of a Dragonfly Wing

by

Teresa Liu

Submitted to the Department of Mechanical Engineering
on May 11, 2007 in Partial Fulfillment of the
Requirements for the Degree of Bachelor of Science in
Mechanical Engineering

ABSTRACT

Insect flight is being studied to aid in the development of micro-air vehicles that use the flapping wing model in an attempt to achieve the high levels of maneuverability that insects have. The flight of the dragonfly has been chosen to be modeled because of its exceptional flight capabilities. This thesis addresses the flapping mechanism designed for the root of each wing. The prototype of the mechanism, built at a scale of four times the size of a dragonfly having a wingspan of 150 mm, is able to create motions in the wing of flapping and feathering, and can vary the stroke plane. The coning angle can be set between tests. The design process began with considering two methods of actuation, a four-bar transmission mechanism used in the Micromechanical Flying Insect developed in the UC Berkeley Biomimetic Millisystem Lab, and by pivoting the wing support directly with cables or rigid links. The second design was chosen to be developed further. A functional prototype was built from acrylic and parts made using stereolithography.

Thesis Co-supervisor: James Louis Tangorra
Title: Postdoctoral Associate

Thesis Co-supervisor: Lynette A. Jones
Title: Principal Research Scientist

Table of contents

ABSTRACT.....	2
ACKNOWLEDGEMENTS	3
TABLE OF CONTENTS	4
1. INTRODUCTION	5
2. BACKGROUND.....	5
2.1 WING OVERVIEW AND KINEMATICS	5
2.2 UNSTEADY AERODYNAMICS AND FLIGHT MECHANISMS.....	8
2.3 EXISTING PROJECTS	9
3. DESIGN REQUIREMENTS	10
3.1 PERFORMANCE CRITERIA.....	10
3.2 DESIGN CONSTRAINTS	16
4. DESIGN PROCESS.....	17
4.1 CONSIDERATION OF TWO METHODS OF ACTUATION	18
4.1.1 <i>Linkage</i>	18
4.1.2 <i>Direct drive</i>	23
4.1.3 <i>Evaluation and decision</i>	31
4.2 DEVELOPMENT OF DIRECT DRIVE DESIGN.....	31
4.2.1 <i>Changing the stroke plane</i>	31
4.2.2 <i>Flapping actuation</i>	35
4.2.3 <i>Cable guides</i>	37
4.2.4 <i>Motor and lever assembly</i>	40
4.2.5 <i>Prototype dimensions and manufacturing</i>	41
4.2.6 <i>Mounting and setting the coning angle</i>	42
5. EVALUATION OF THE PROTOTYPE AND FURTHER IMPROVEMENTS	43
APPENDIX A.....	50

Acknowledgements

I would like to thank Dr. James Tangorra and Dr. Lynette Jones for giving me the opportunity to work on this project and for their guidance throughout the semester. I would also like to thank members of the BioInstrumentation Lab who assisted me with various tasks around the lab, and fellow mechanical engineering students who have offered their time in aiding me throughout the semester. Finally, I would like to thank my family, friends, and sisters for their support this semester and during my time at MIT.

structure and strength to the wings, and likely contribute to the flexibility of the wing depending on how much blood is contained in the veins. Each wing has a leading edge, which is stiff, and a trailing edge that is more flexible (Combes and Daniel, 2003). The wing is connected to the body at a joint which is driven by several muscles. There are posterior and anterior wing elevators and depressors, as well as muscles to pronate the wing and restore the shape of the notum, the dorsal part of the thorax, which deforms with wing movement (Clark, 1940).

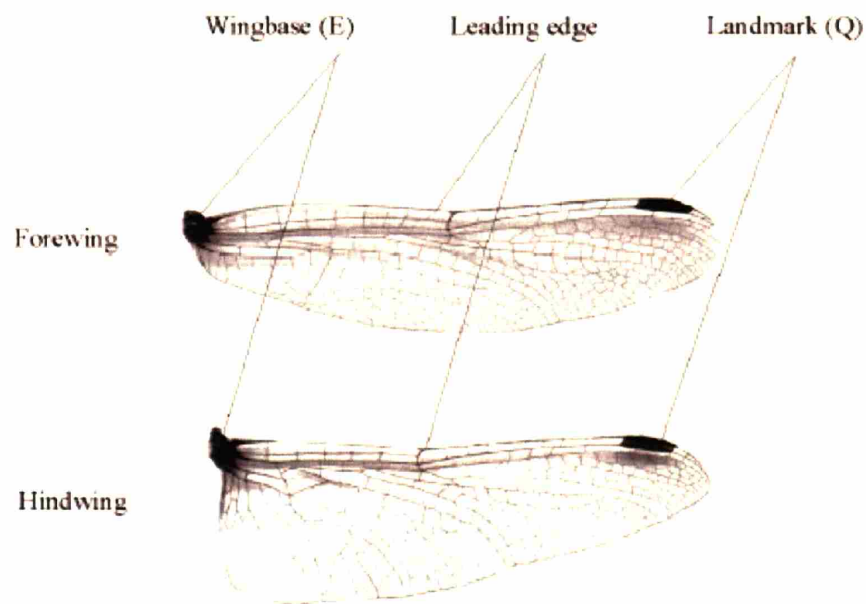


Figure 1: Forewing and hindwing of a dragonfly. (From Wang et al., 2003)

Insect wingstroke varies depending on the insect and the flight mode. Insects often trace a figure eight shape with the tip of their wings, especially in hover (Wang, 2005). Stroke plane may be horizontal or inclined in hover, and in moving forward often the stroke plane becomes more inclined (Sane, 2003). The inclined stroke plane is shown in Figure 2. In the dragonfly, different studies give different shapes traced by the wingtips (Azuma, 1985), possibly due to the variety of flight modes studied and also due to the difficulty in recording movements in free

1. Introduction

Insect flight is being studied to assist in the development of micro air vehicles (MAVs). Micro air vehicles are small aircraft less than 150 mm long, that are being developed primarily for use in hazardous environments such as in military applications and in collapsed buildings. Three common types of MAV are the fixed wing model (e.g. plane), the rotating wing model (e.g. helicopter), and the ornithopter model. The ornithopter uses flapping wings in imitation of birds and insects since flapping motion can often achieve higher maneuverability than a fixed wing. Birds and insects both have significant flight capabilities that would be desirable in a micro air vehicle; however, insects are simpler than birds in many ways in the movement of their wings and thus are easier to model. Wing motions in insects are actuated only at the base, with no muscles extending into the wing itself.

The goal of this project is to build a mechanism replicating the motions at the base of the wing that allows the study of the fluid flow and forces created by different flapping motions. This information will be useful for the incorporation of various motions into wings of MAVs to provide more efficient flight. The dragonfly has been chosen as the focus of study for this study. The dragonfly in particular exhibits ideal flight capabilities for an MAV; it can hover and has high maneuverability: it can glide, fly sideways, turn quickly, and fly in windy environments.

2. Background

2.1 Wing Overview and Kinematics

Insects have flexible wings that grow out of the thorax and are actuated by muscles at the root of the wing. Dragonflies have four wings—a pair of forewings and a pair of hindwings. The forewing and hindwing are shown in Figure 1. Throughout the wings there are veins that give

flight accurately. The shape traced by the wingtip is generally a narrow figure eight in the dragonfly (Wakeling and Ellington, 1997). An example of the wingtip path for the dragonfly *Sympetrum sanguineum* is shown in Figure 2. The stroke plane is roughly perpendicular to the direction of travel; a dragonfly hovers with an inclined stroke plane (Wang, 2005), and as it climbs the stroke plane becomes flatter relative to the horizontal (Wakeling and Ellington, 1997). The dragonfly's fore and hindwings typically counterstroke, or beat out of phase. During take-off and hovering, when greater lift forces are needed, the wings beat in phase (Alexander 1986). In turning, the dragonfly has high maneuverability due to the four wings' ability to flap independently. In just a few wingbeats a dragonfly can make a quick turn by varying, for example, the stroke angle and phase relationships of its wings (Alexander 1986).

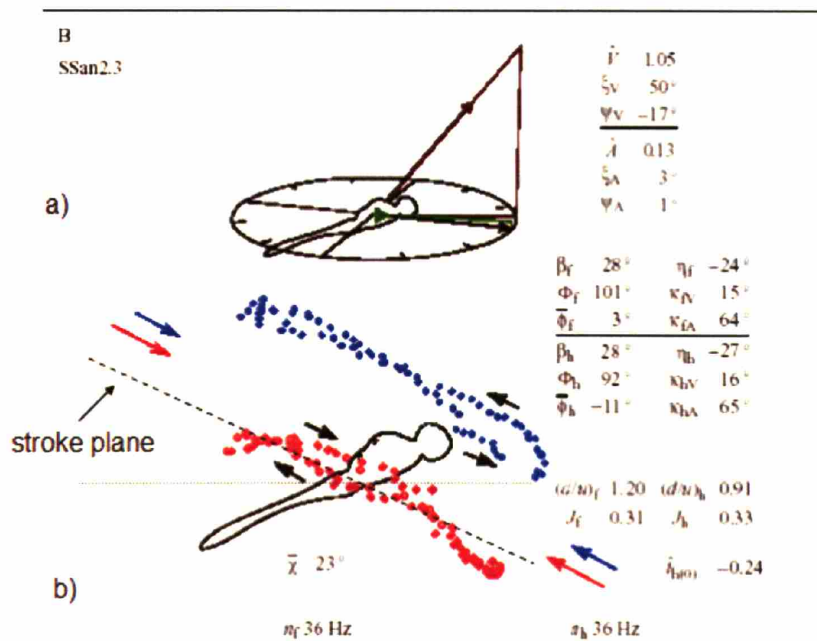


Figure 2: An example of a wingtip path for dragonfly *Sympetrum sanguineum*. The short arrow in (a) originating from the body is the acceleration vector, and the two long arrows indicate velocity. The inclined stroke plane is shown in (b). (From Wakeling and Ellington, 1997).

2.2 Unsteady aerodynamics and flight mechanisms

The understanding of insect flight has gone through significant development in the past few decades. Research has shown that by using steady aerodynamics the lift coefficient required for insects to fly was unrealistically high, around 3.5 to 6.1, and so further research took unsteady effects into account (Sane, 2003). Previously it was assumed that the air flow over a flapping wing was the same as the air flow over a non-flapping wing with the same angle of attack; however, aerodynamic forces change magnitude and direction through each wingbeat (Zbikowski et al., 2005). This study of unsteady aerodynamics has been the focus of most current research in insect flight.

In the study of unsteady aerodynamics, proposed flight mechanisms in insects include delayed stall, rotational circulation, and wake capture (Sane, 2003). In delayed stall, the wing has a large angle of attack. In a non-flapping model of a wing, vortices form on the leading and trailing edges and shed as it continues to translate, which causes the wing to lose its lift. In a flapping wing, however, a vortex at the leading edge remains as the wing translates, providing lift to the wing. In rotational circulation, lift is produced from the rotation of the wing at the end of a stroke. Rotating about the trailing edge produces a leading edge vortex, and the timing of the rotation is essential to the forces produced. Wake capture takes advantage of the previous stroke's vortices, creating additional lift. Reversing the wing stroke sheds the leading and trailing edge vortices, creating a stronger velocity field, which the wing then encounters. None of these three mechanisms alone can account for the total lift generated through flapping flight.

2.3 Existing Projects

Due to the difficulty of studying complex insect aerodynamics in nature, researchers have developed flapping mechanisms that model either the wings and the thorax together, or just the wings by themselves. The models allow for easier measurement and analysis of various aspects of flight such as the forces on the wing, forces due to wing motion, and the flows created by the flapping wings.

Ellington et al. (1996) and Dickinson et al. (1999) developed models of the hawkmoth and fruit fly respectively. Ellington created a scaled up flapping device that modeled a hovering hawkmoth's wing motions, called 'the flapper,' which he used to look at vortices created by the wing stroke (Van Den Berg and Ellington, 1997). From their experiments they determined that the leading edge vortex created on the downstroke was the primary provider of lift force. The model itself was ten times the size of the hawkmoth, flapped at one hundredth of the hawkmoth's wingbeat frequency in order to maintain the Reynolds number, and used servo motors to drive the gears that moved the wings. Dickinson et al. (1999) also developed a scaled up model of the fruit fly in order to study the effects of the timing of stroke reversal on lift generation over the course of a wing stroke. They also measured the aerodynamic forces and recorded the flow around the wing using digital particle velocimetry. This enabled them to characterize the motions of the generated vortices (Birch and Dickinson, 2001).

Both Ellington et al. (1996) and Dickinson et al. (1999) used scaled up models of insects, modifying wingbeat frequency to stay within the correct Reynolds number range. However, in a scaled up model the correct Strouhal number, the dimensionless number characterizing oscillating flow mechanisms, is not maintained (Zbikowski et al., 2005), and so the results may

not be accurate. The model developed in this project will be on the same scale as a dragonfly, keeping both the same Reynolds number and Strouhal number.

Fearing has been working on the Micromechanical Flying Insect (MFI) since 1998, which is manufactured at a smaller scale, with a wingspan of 25 mm. It is modeled after the blowfly, *Calliphora*, which has a wingspan of 11 mm and a wing beat frequency of 150 Hz. Like insects such as blowflies and fruitflies, the MFI drives the wings at mechanical resonance in order to avoid losses in energy. The wing apparatus was also designed to provide adequate wing rotation in recognition of the importance of wing rotation, particularly at the end of the stroke, in generating lift (Yan et al., 2001). They mapped lift and thrust forces of a 2 DOF wing, using a precision balance to record data during flapping (Yan and Fearing, 2003).

This research gives valuable insight into the flight aerodynamics of insects. The project to be undertaken by the MIT BioInstrumentation Lab will incorporate the use of advanced software for computational fluid dynamics, which will enable researchers to better characterize fluid flow around the wing. Past models and algorithms have attempted to use computational methods to calculate forces generated by wings, but need more improvement for theoretical values to better match experimental results (Yan and Fearing, 2003). This project will make use of an advanced model of a flexible wing structure that deforms with flow, something that has not yet been encountered in literature.

3. Design Requirements

3.1 Performance Criteria

The final design should meet several performance criteria based on what is known about dragonfly kinematics from the literature. Past studies have varying degrees of detail and scope,

and so performance criteria were chosen by looking at several sources and sometimes extrapolating to determine information that was missing.

- The prototype wings should have a flapping amplitude range of 120-180 degrees which is symmetrical about the horizontal. Ideally each wing should have a range of motion of 160 degrees, 80 degrees above and below the horizontal. If necessary, the range of motion can be reduced to 120 degrees. Typical flight in dragonflies requires up to 100 degrees (Ruppell, 1989), with greater amplitudes in high lift situations such as during vertical take-off and carrying a female during mating (Ruppell, 1989). However, because the neutral axis may be below the horizontal (Figure 3), greater amplitude below the horizontal is needed to achieve the appropriate range of motion. No specific angle for the neutral axis has been found in literature; an estimate of 10 degrees below the horizontal has been obtained from Azuma (2006). A flapping amplitude of 180 degrees about the horizontal should be adequate for reaching normal flight conditions while allowing for some flexibility in changing the neutral axis.

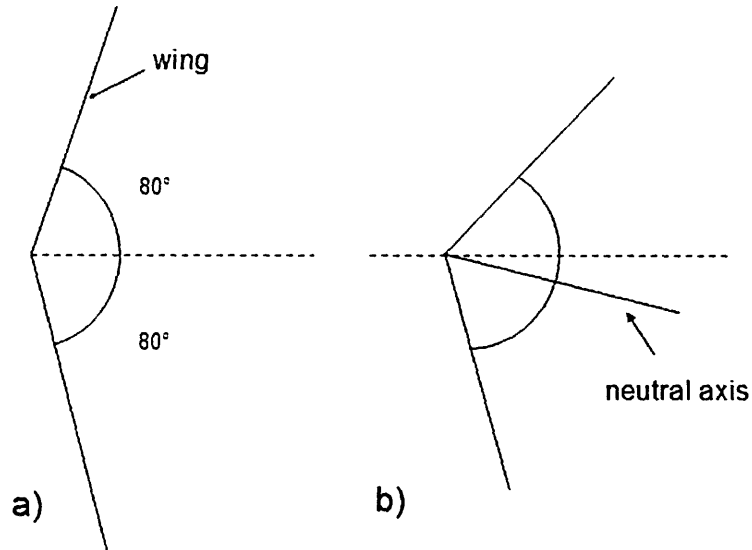


Figure 3: The device should have a flapping amplitude of 160 degrees, 80 degrees above and below the horizontal (left). The neutral axis of flapping may be below the horizontal (right).

- Each wing should be able to feather 60 degrees above and below the horizontal about its long axis, defined as the line passing through the quarter-chord of any cross section of the wing. This axis lies roughly halfway between the two wing joints, which operate independently of each other, enabling the wing to rotate about its leading or trailing edge. The phase difference between the two joints creates the feathering angle of the wing; the greater the phase difference, the greater the angle. Figure 4 shows feathering of a dragonfly wing in a tilted stroke plane.

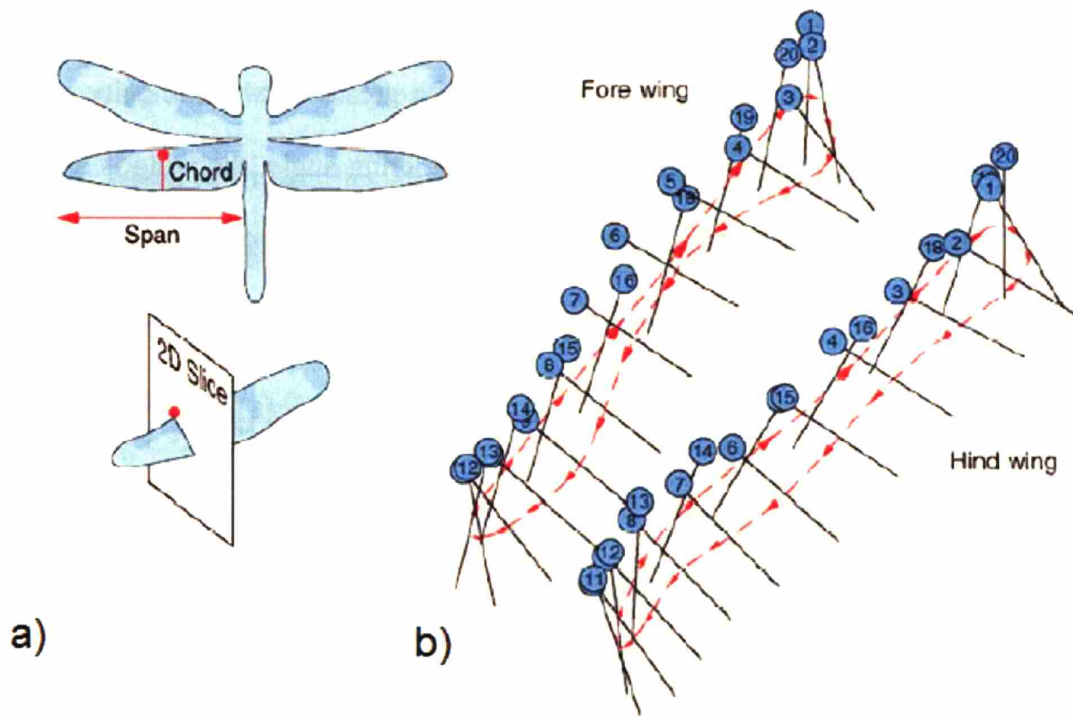


Figure 4(a): The wing is sliced along a chord length, with the circle indicating the leading edge. 4(b) shows the path of a slice of the dragonfly wing as it feathers in a tilted stroke plane. (From Wang, 2005)

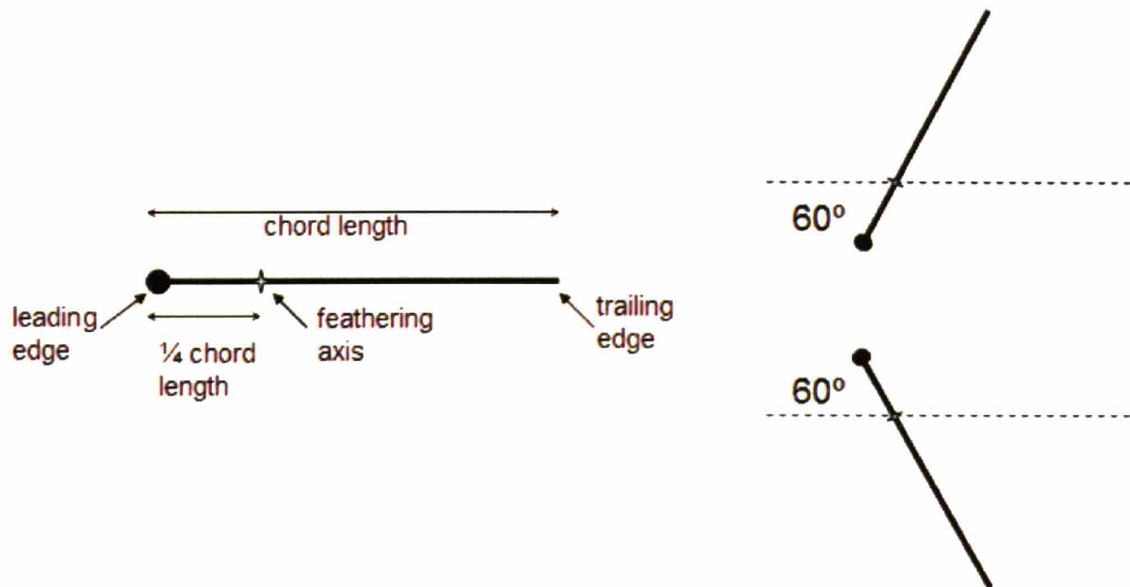


Figure 5: The wing should rotate 60 degrees above and below the horizontal about its long axis (or feathering axis)

- Wings beat in a stroke plane of 40-70 degrees above the horizontal (Azuma, 2006).

The stroke plane is defined as the plane in which the wing moves in one stroke. A

wing stroke extends from behind and above the joint to before and below the joint. The angle of the stroke plane increases with greater forward velocity and decreases with greater vertical velocity. At zero feathering angle, the wing is assumed to be angled 20-50 degrees from the horizontal since the plane of the wing is perpendicular to the stroke plane (Figure 6)

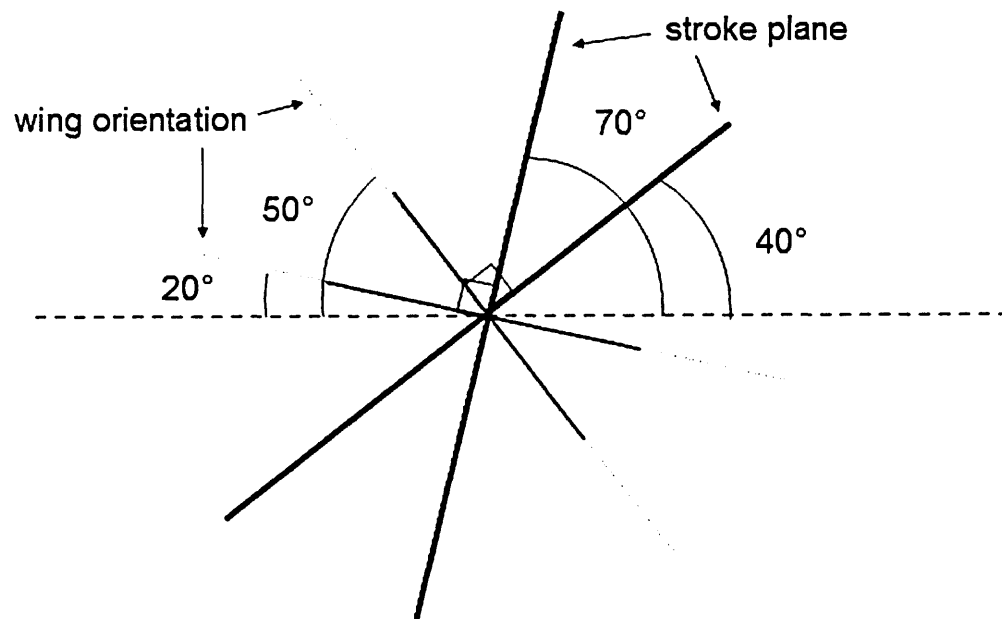


Figure 6: The stroke plane varies from 40 to 70 degrees from the horizontal, and the corresponding plane of the wing varies from 20 to 50 degrees from the horizontal

- Wings should beat at a frequency of about 40 Hz, with one cycle defined as an upstroke and a downstroke. Studies have recorded various frequencies for the beating of dragonfly wings such as about 30 Hz in Azuma (2006) and 44 Hz in Ruppell (1989).
- Dragonfly wing velocity varies throughout the stroke, and the maximum velocity may be greater than that estimated from a simple sine wave with appropriate

frequency and amplitude. The prototype should be able to create velocity profiles for the wing other than a simple sinusoid.

- The wings of dragonflies are not perfectly perpendicular to the body. The coning angle, or the angle of the wing to the body in the yaw direction should be adjustable. The forewing is generally angled about 10 degrees forward, and the hindwing about 2 degrees back (Azuma, 2006).

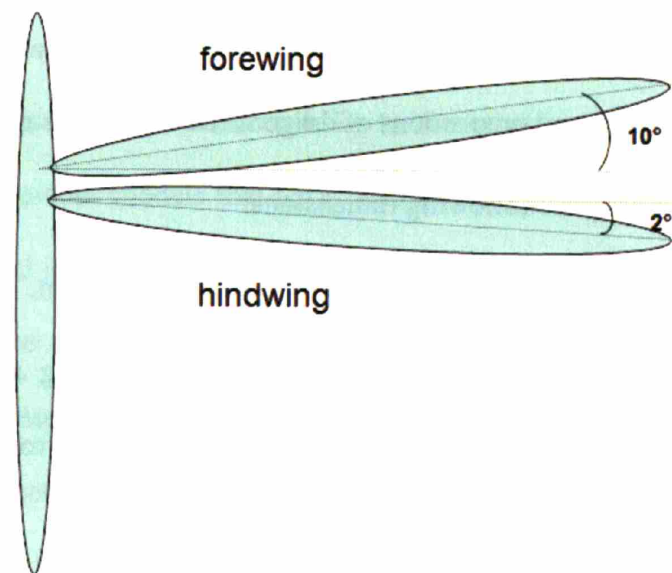


Figure 7: The forewing is angled about 10 degrees forward, and the hindwing is angled about 2 degrees back

- The flapping mechanism should be able to operate for at least ten minutes without failing, an estimate of how long is necessary for adequate testing and data collection.

In choosing these performance criteria, more range of motion has been specified than the dragonfly may have. Since many specific criteria are unknown, it was considered desirable to allow more degrees of freedom to enable exploration of the effects of various motions. Dragonfly anatomy was used for insight into how a dragonfly wing is actuated (Neville, 1960; Simmons, 1977; Wootton, 1992).

3.2 Design Constraints

The goal in designing the flapping device is to test the aerodynamics of flapping motions, so the device should be encased in a housing that is similar to body of a dragonfly. The housing should be close in size to a dragonfly thorax, and should not impede air flow past the wings.

The flapping mechanism is for a robotic dragonfly with a wingspan of 150 mm. A rough estimate of the body's dimensions was obtained by looking at photographs of dragonflies and scaling the bodies and wings up to 150 mm wingspan. There is some freedom here to vary the dimensions since the sizes and proportions of dragonflies vary across species.

The body should have the following dimensions:

- The distance between two joints of one wing is 2.5-3 mm.
- The distance between the hind joint of the forewing and the fore joint of the hindwing ranges from approximately 3 mm estimated from photos to 8.2 mm from one particular paper by Azuma et al. (1985).
- The width of the thorax casing is about 10 mm.

Because of manufacturing limitations in the time available for building the prototype, the actual dimensions of the prototype are four times the dimensions specified.

The housing containing the flapping mechanism can be tall as long as it remains stable. The housing can be broader at the base as long as it does not interfere with the air flow created by the wings. The minimum distance the base can be from the wing attachment point is 66 mm in order to clear the wing, assuming a length of 70 mm, but there should be additional space in the final mechanism so that air flow is not disrupted.

The torque required to flap a dragonfly wing was estimated by adding the peak torque due to drag and the peak torque due to rotational inertia, using maximum stroke velocities obtained by Ruppell (1989) for various species of dragonflies. The maximum stroke velocity may be different from a velocity calculated from a simple sine wave representing the vertical position of the wing. The maximum torque calculated was about 6.2×10^{-3} Nm (see Appendix A).

4. Design Process

A literature review was first conducted in order to see what models had previously been developed. Many of the previous models that have been developed were scaled to a size much larger than that of the actual insect (Zbikowski et al., 2005), enabling the model to employ more complicated mechanisms to move the wing. One model that was scaled accurately was the Micromechanical Flying Insect (MFI), developed in the Biomimetic Millisystem Lab at UC Berkeley, which had a wingspan of 25 mm and was capable of flight (Zbikowski et al., 2005). Each wing flapped using a four-bar linkage mechanism. Because the MFI was one of the few devices that was on the same scale as an insect, it was examined more closely in order to determine what could be learned from it. Other designs used gears and transmissions that were difficult to miniaturize.

In determining the final mechanism used to flap the wing, I considered the four-bar linkage inspired by the MFI design as well as a mechanism using cables or rigid links to drive the flapping motion directly. Models of both methods revealed the capabilities of and issues associated with each. After examining each method, one approach was chosen to be developed further.

4.1 Consideration of two methods of actuation

4.1.1 Linkage

The linkage in the MFI served as the starting point for developing one method of flapping the wing. Goals in developing models were to analyze the benefits of using a linkage and to determine if a linkage was appropriate for this project's purposes.

4.1.1.1 MFI design

In the MFI, each wing is flapped using a four-bar linkage as shown in Figure 8. There are three bars 6 mm long, and a short bar 0.5 mm long. The wing is connected to a spar which lies on the shortest bar. Points C and F are fixed, and Point B is actuated by the PZT actuator at A. An approximately linear horizontal motion at point B translates to a maximum of 180 degrees of rotation for the spar.

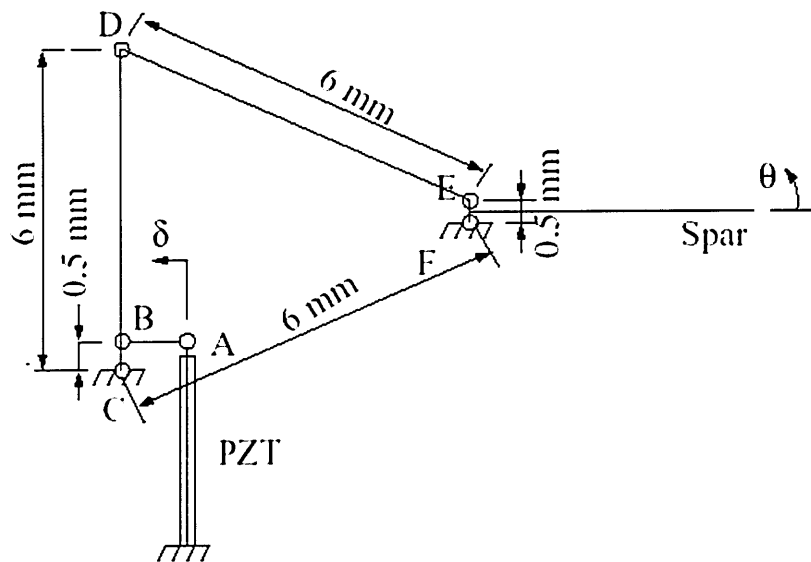


Figure 8: Linkage used to drive the wings of the Micromechanical Flying Insect. A PZT actuator drives the rotation of the spar (From Yan et al, 2001).

There are a few aspects of the linkage in the MFI that are not ideal for this project and would need to be modified. The wing has an arcing pivot point since the wing spar is attached to the midpoint of a bar (EF) that rotates about an endpoint (F), shown in Figure 9. This arc is small, but is not desirable in reproducing the motions of a dragonfly wing, which probably has a stationary pivot point. The exact linkage in the MFI also does not meet the design constraints for this project since it extends too far into the body to fit a pair in a 10 mm wide thorax.

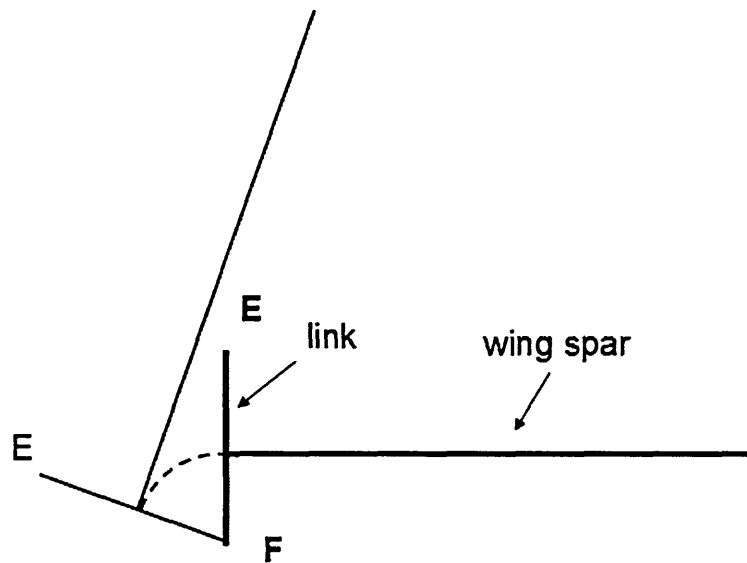


Figure 9: Due to the attachment of the wing spar to the midpoint of the link, the end of the wing spar travels through an arc instead of remaining stationary.

4.1.1.2 New Linkage

In examining the four-bar linkage design as a possible path, I first focused on how to achieve flapping and feathering since changing the stroke plane and setting the coning angle would be fairly independent from flapping and feathering. If no alternative was found, the stroke plane could be changed by rotating the platform on which the motors rested, and the coning angle could be set by rotating an additional platform underneath.

To be appropriate for this project, the wing support should have a stationary pivot point, and the linkage should fit the design constraints. The attachment point of the wing spar was first moved from the middle to the secured end of the shortest bar where rotation occurs so that the wing spar rotates about a stationary pivot point (Figure 10). Since the linkage is slightly larger than what is appropriate for the dragonfly body, the linkage lengths need to change in order to fit within a smaller footprint while giving a flapping amplitude of 160 degrees. Given a thorax width of about 10 mm, each flapping unit should not extend more than half the width, or 5 mm, into the body. In the MFI, half the linkage also extends above the wing joint. Since in a dragonfly the top of the wing appears to be flush with the top of the thorax, the flapping mechanism for this project would ideally be contained below the wing joint, keeping the air above the joint undisturbed.

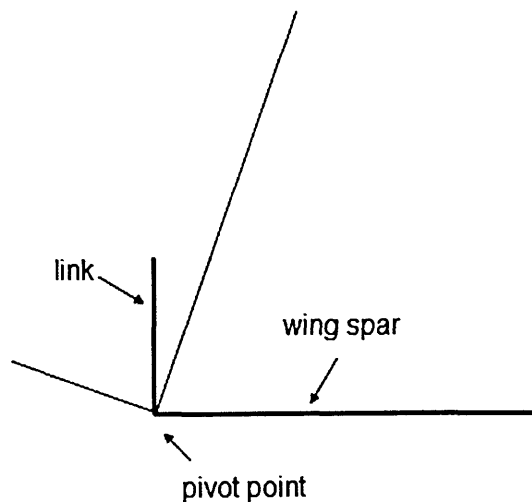


Figure 10: Attaching the wing spar to the endpoint of the link gives the wing a stationary pivot point.

To determine a linkage that would meet these space constraints and manufacturing limitations, and still achieve appropriate flapping amplitude, I experimented with different relative linkage lengths and different orientations. The goal was to minimize the angle of rotation

necessary in the driving bar to move the wing through its full range of flapping while staying within space constraints. In Figure 11, A is fixed, B is actuated, and the wing support is connected to the end of D that attaches to A. The configurations of the links at the two extremes of the flapping range are shown. When the wing is at its highest point, links C and D are collinear. When the wing is at its lowest point, links A and D are collinear. It is possible to move the wing higher by continuing to rotate link D counterclockwise, where C and D create a concave angle, but there is no way to control which direction D rotates by controlling link B. Thus, the point at which C and D are collinear is at the extreme. It is also possible to rotate D clockwise past the configuration shown to achieve a greater angle below the horizontal, but it is preferable not to extend into the space above the wing.

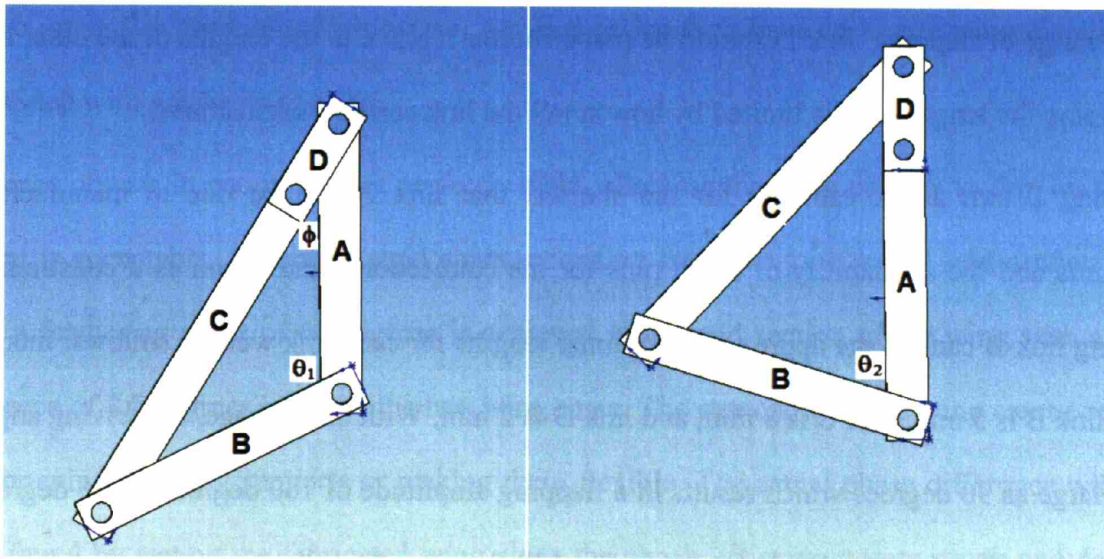


Figure 11: Orientations of four bar linkage at two extremes.

Calculations were done using the law of cosines. In the first configuration, where C and D are collinear, the angle ϕ is the supplementary angle to the full flapping amplitude. The angle θ_1 is the starting angle for the driving link B. Link B ends with angle θ_2 . $\Delta\theta$ is the angle necessary

to drive the wing spar through an angle of $(180-\phi)$ degrees. ϕ and θ are calculated using Equations 1-3.

$$\cos\phi = \frac{(C+D)^2 + A^2 - B^2}{2A(C+D)} \quad (1)$$

$$\cos\theta_1 = \frac{(A^2 + B^2) - (C+D)^2}{2AB} \quad (2)$$

$$\cos\theta_2 = \frac{(A+D)^2 + B^2 - C^2}{2B^2(A+D)} \quad (3)$$

To minimize the number of variables, links A and B were set to have the same lengths in initial calculations. These calculations showed that the longer link C is relative to the lengths of links A and B, the greater the flapping amplitude. To reduce the rotation of B needed to obtain the full range of flapping, link D should be made shorter relative to the lengths of the other links. Minimizing the length of D is limited by how small the link can be manufactured.

Using 2 mm as an estimate for the shortest that link D can be due to manufacturing constraints and the availability of small pins for the connections, and 5 mm as a constraint for how long link B can be, the approximate optimal lengths for each link were as follows: link A is 5 mm, link B is 5 mm, link C is 8 mm, and link D is 2 mm. With this linkage, the driving angle is still as large as 90 degrees which results in a flapping amplitude of 160 degrees, or 75 degrees if the maximum flapping amplitude is reduced to 140 degrees. At a distance of 1 mm away from the pivot point of link B, the side to side linear displacement needed is 1.4 mm. Piezoelectric actuators typically displace less than 1 mm, so using a piezoelectric actuator is not a viable option.

Link B can be driven by a pulley system that will further gear down the angle. Cables attached to both sides of link B will pull it in alternating directions. This achieves the amplitude

required, but includes gearing in two steps which may not be necessary. Link B can also be driven by a linear actuator that will push and pull from one side. Because the motion at any one point on link B is not linear but is actually an arc, the driving arm will need to either rotate with respect to the actuator and link B, or be slotted so that the interface with the link can slide. Using this method, the translation of linear motion into rotary motion will need to be accounted for in the mathematics for actuating the arm.

4.1.1.3 Interface with wing

If two joints per wing are used with stiff spars moving out of phase, the distances between the two wing supports changes. One option to address this issue is changing the distance between the two joints so that the joints flex inward as the phase difference increases and back out when the two joints flap more closely in phase. Another option is to have an elastic wing material that will stretch with greater feathering.

Since objects in nature are not perfectly rigid, allowing the wing or joint to flex by a small amount is acceptable. Assuming rigid spars extending from the joint to the mid section of the wing, a feathering angle of 60 degrees is achieved at the mid section of the wing with a phase difference of 8.5 degrees between the two wing spars. The stretching of the wing can be reduced by shortening the wing supports or making them flexible. The actual phase difference will need to be found by testing the fabricated wing since the above estimate is very rough and does not account for the flexing of the wing. With each wing of different flexibility, a different phase difference will be associated with the feathering angle.

4.1.2 Direct drive

Several designs using cables or rigid links were considered and prototyped in the development of the direct drive method. The initial designs included a rigid wing base, with two

wing supports rigidly connected so that they remained in the same plane. Feathering could be induced by angling the two joints at the base of the wing. Each wing needed to pivot about a point that could rotate in three directions.

4.1.2.1 Cables

The first design used a set of cables to flap the wing and used one motor to drive the flapping of the wing. As the wing is pulled down, the bar on the other side of the pivot pulls the cable up, and vice versa. This reduces the need for two motors to pull the wing support on opposite sides of the pivot point to one motor that pulls both sides of the wing. Figure 12 shows a side view of the pulley and wing system.

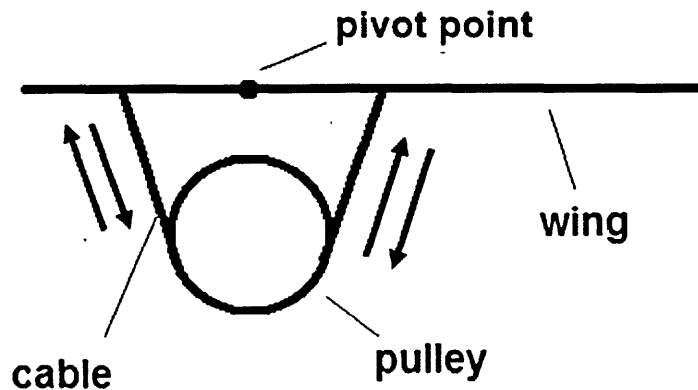


Figure 12: Diagram of cables actuating the wing support. The pulley rotates around a fixed point, and the cable pulls on the wing support on either side of the pivot. Rotating the pulley will shorten the cable on one side and lengthen the cable on the other.

The pulley also pivots about its midpoint to create a feathering motion. Figure 13 shows the wing and pulley system from the rear. As the pulley rotates, the cables cause the wing to rotate to the same angle. The midpoints of the pulley and the wing stay fixed.

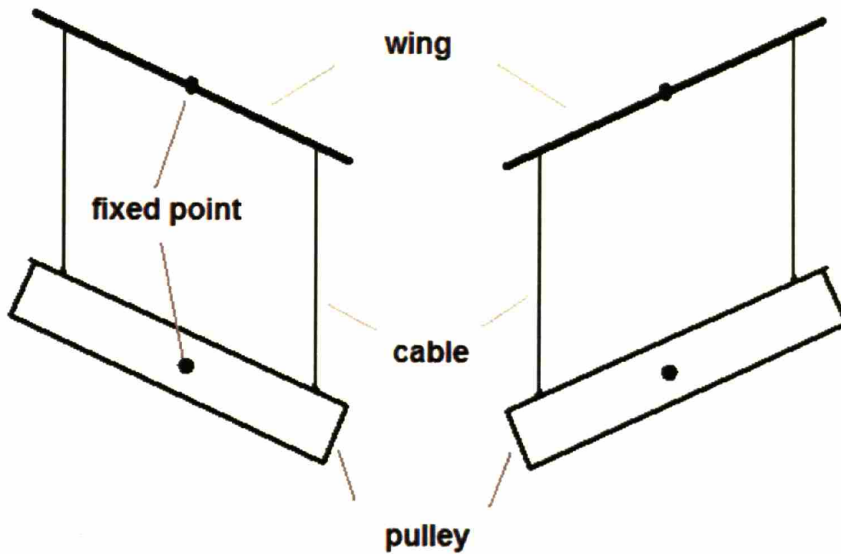


Figure 13: View from the back of the wing, looking out across the wing. The pulley rotates about a fixed point to change the feathering angle of the wing.

One issue with this design is that the cables are connected to the pulley at an angle, causing it to spool across the pulley instead of remaining on one circumference (shown in Figure 14). The pulley can be grooved, or the pulleys can be separated so that they remain horizontal and perpendicular to the cable (Figure 15). If there are two separate pulleys, two separate motors will be required to drive each one.

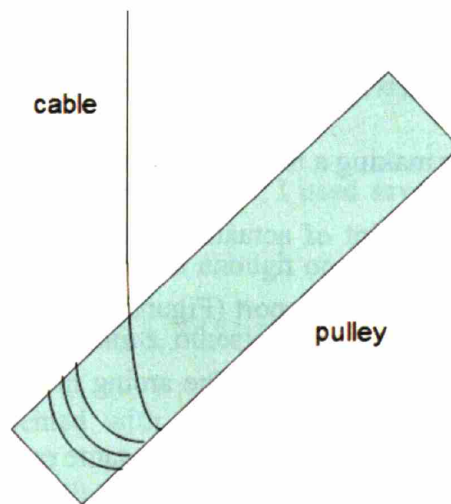


Figure 14: Angling the pulley causes the cable to wrap around at an angle.

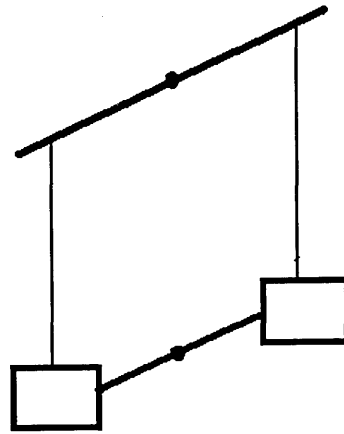


Figure 15: Instead of a single pulley for both joints of the wing, the pulleys are separated in order to keep the cables perpendicular to the pulleys.

In using cables to pull on the wing support, one should consider the distance between the attachment of the cable and the pivot point. The further out the cable extends into the wing, the more likely it is to disrupt the air flow created by the flapping motion, making rigid links on the inside half of the wing support a better option. However, this may not be an issue at all, since the wing's rotation translates into a small linear distance close to the root of the wing, and the air flow where movements are small is probably not essential to the total forces created by the wing.

4.1.2.2 Rigid links

The second design for a rigid wing involves rigid links instead of cables. Two links push and pull on the two supports. After making a mock-up of this design, it could be seen that there was a lot of movement needed at the point of actuation, assuming vertical links. There is an arcing motion due to the rotation of the wing support (Figure 16). There is also a movement in towards the feathering axis due to feathering motion. The arcing motion can be addressed by attaching the links to something that also travels in an arc of the same radius, such as a wheel. The distance traveled towards the feathering axis is small and could be addressed by a pivoting motion at both

ends of the link. However, this would also introduce an additional factor to consider in calculations in controlling the actuators.

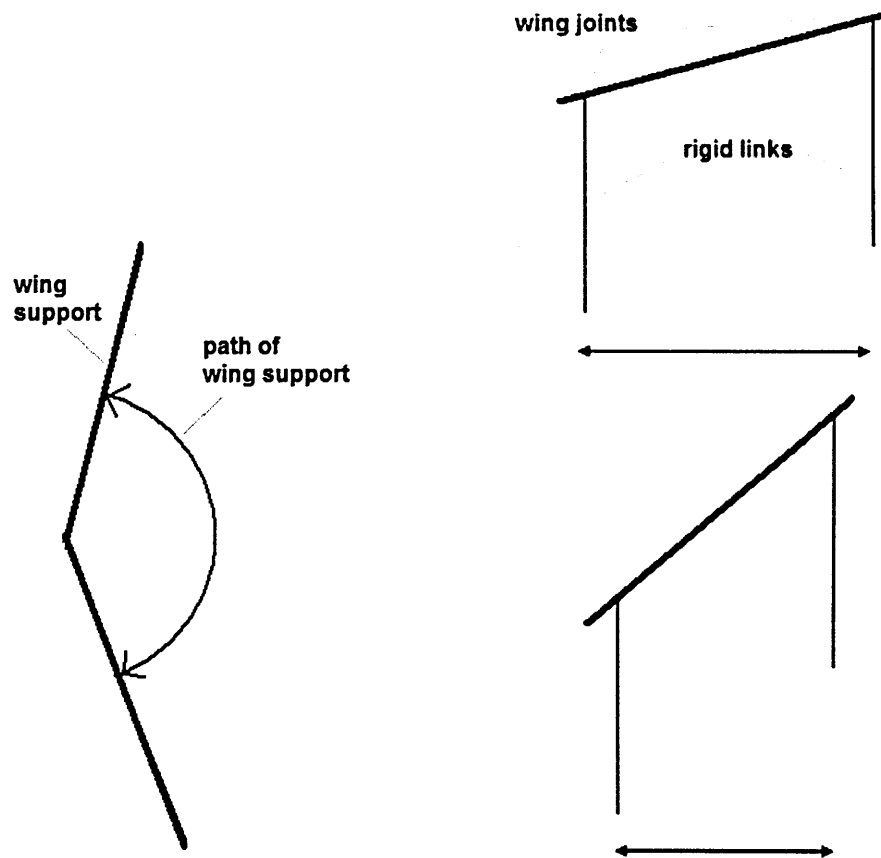


Figure 16: The wing support traces an arc as it flaps, requiring the same motion from the rigid link driving it (left). As the feathering angle increases, the links will need to move closer together (right)

4.1.2.3 Ball joint designs

In mocking up scaled up models of the designs, I used several different materials to make the joint. Since there were no ball joints small enough or with a large enough range of motion that I could obtain within the time constraints, other materials were used.

The first material I experimented with was Smooth-On urethane rubber, (ReoFlex and Evergreen Series, Smooth-On, Inc., Easton, PA), used as molding material that can flex and stretch. A stiff vertical rod and a horizontal rod or plate connected with elastic material would

allow rotation in three directions. Figure 17 shows different designs using the urethane rubber. In working with the material, it was difficult to make intricate shapes on a small scale. Another issue with designs a-c was that the center of the wing pivots around a point outside the joint due to its arcing motion.

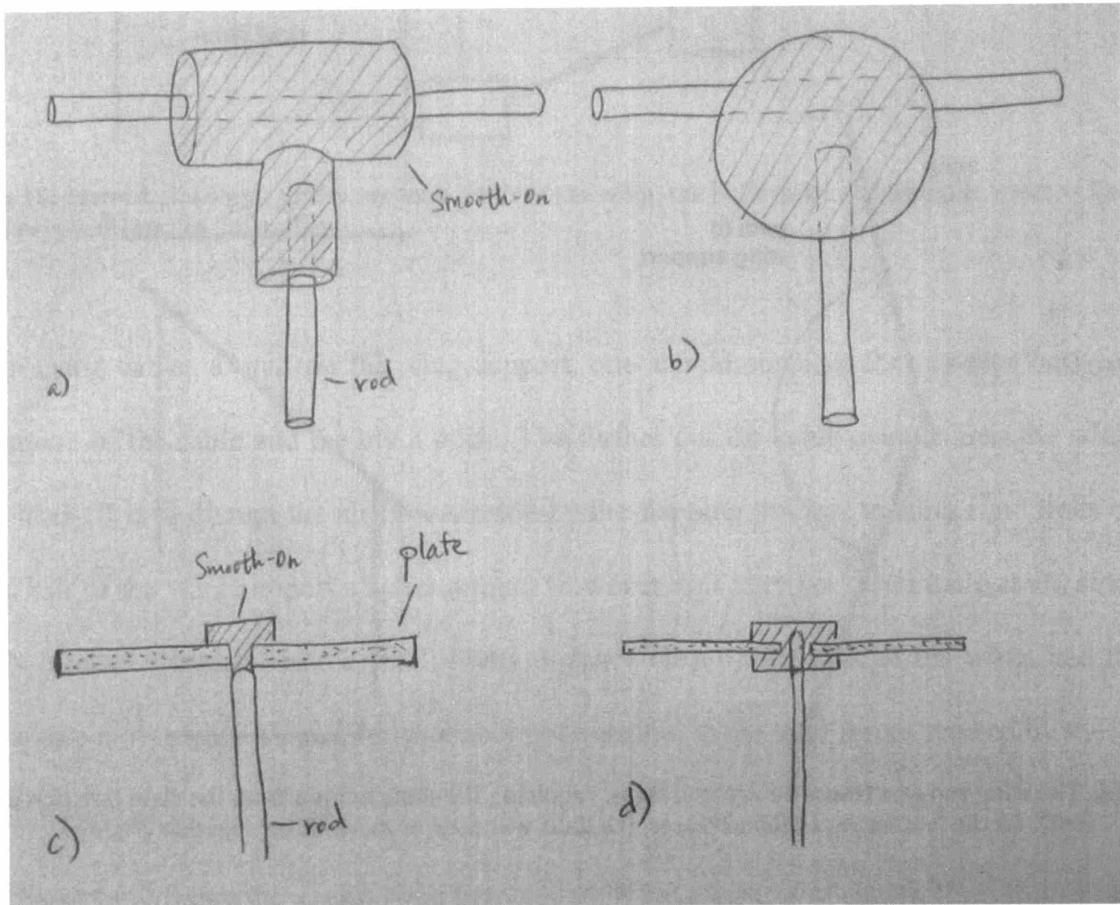


Figure 17(a-d): Back view of various joints using a combination of rods, a plate, and urethane rubber. Figures 17c and 17d show a cross sectional view. The wing supports lie on the ends of the horizontal rods and the sides of the plates (not shown)

One simple option for a flexible joint involved a cylinder through a hole in a plate holding the wing supports. Since all the glues used on the urethane rubber could be peeled off, the only way to secure the cylinder to the plate was to pour excess material around the hole. (Figure 17d) After making the joint, it was noted that the rubber was fairly weak when only a small amount

was applied. The hole in the plate would also need to be fairly large in order to accommodate the range of motion necessary for flapping (Figure 18), making the joint less stable.

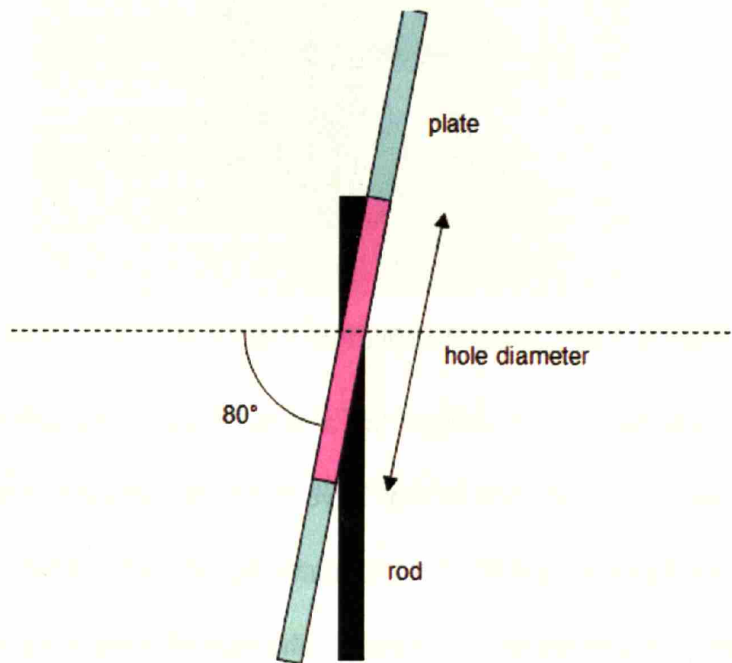


Figure 18: Side view of wing. The wing flaps 80 degrees above and below the horizontal, so a hole that allows a rod to pass through would need to be wide.

Since a ball joint could not be manufactured easily, a joint was made by applying epoxy to nuts and bolts which allowed rotation in three directions. This served the purposes of the mock-up, but is not ideal since the rotations do not occur at the same point. Miniaturization would also be difficult.

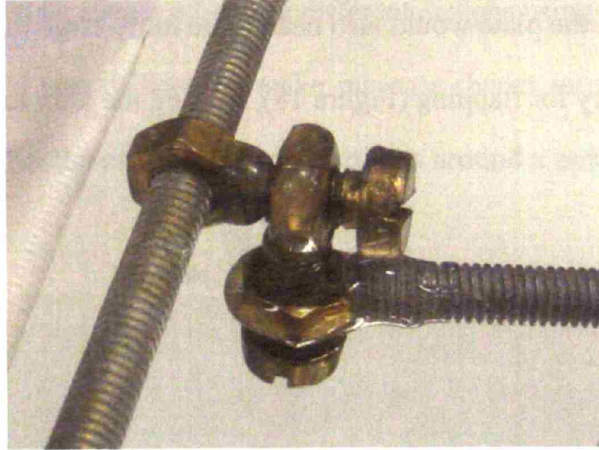


Figure 19: A joint with three degrees of freedom made from nuts and bolts

The ball joint included in the design for a wing presents several issues. The first is manufacturability. There may be options that have not been explored, but the design options explored in this project have been difficult to miniaturize, not very robust, and/or reproduce the kinematics inaccurately due an arcing pivot point. The second issue is the constraint in degrees of freedom. If the wing joint is rigid and fixed at one point, and each wing support is constrained to travel parallel to the stroke plane, then the movements of the two wing supports are coupled. With a single ball joint in the middle of the wing joint, the wing always feathers about a chord containing the ball joint. The wing cannot hold one joint still while moving the other. However, it is ideal for the wing joints to move independently. Each joint is actuated by separate muscles, so it is logical that they move independently from each other with some degree of coupling due to the attachment to the same wing. Further iterations of the direct drive method of actuation should drive each joint independently.

4.1.2.4 Interface with wing

The original intent of having a rigid wing for the direct drive was to avoid the need to stretch the material of the wing. However, as discussed in the section 4.1.1.3, the issue of the wing material stretching is allowable since it stretches by a small amount, and is probably what real

wings do at the base. Further designs using the direct drive method of actuation will use the same interface as the linkage design.

4.1.3 Evaluation and decision

The decision was made to pull directly on the wing supports and not to use linkages to drive the flapping of the wing. Both methods would produce the appropriate kinematics given no space limitations, and so the decision was based on space constraints, simplicity of design, and manufacturability. A linkage would occupy more space since it would need to be connected to another mechanism that would drive the movement of one link. Having two mechanisms instead of one is also not ideal when one mechanism alone would suffice.

Benefits to the linkage include the ability to achieve resonance to flap at higher frequencies using less power, and the possibility of having a smaller flapping unit. This was necessary for the MFI since it needed to fly. These characteristics are not necessary for this project, since the unit will not fly and can use actuators that are much larger and provide more power. The frequencies of flapping required are also much lower—40 Hz for this project compared to 139 Hz for the MFI (Yan et al., 2001).

4.2 Development of direct drive design

4.2.1 Changing the stroke plane

The original method of changing the stroke plane was to swing the platform holding the flapping device, including the actuators. However, this was cumbersome and required a lot of space. Since there is a certain amount of space that should be left open below the wing joint to

allow for the wing to flap down, the connections of the flapping mechanism to the motors below would need to be even larger to give room for the motors to swing up.

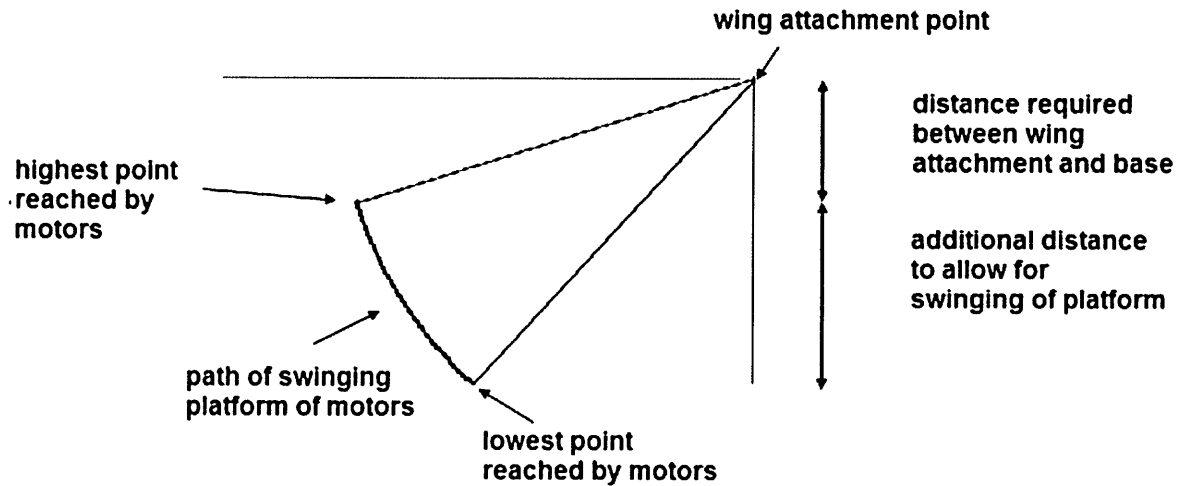


Figure 20: Diagram of swinging motors system to change the stroke plane. Swinging the motors requires more height in order to accommodate the path of the motors while maintaining free space around the wing.

A method of changing the stroke plane that does not require rotating a lot of equipment through a large arc would be preferred. The two joints should rotate about a middle point to produce a rotating stroke plane without the connection moving with the wing. One way to do this is to change the relative heights of the joints, keeping the pivot point stationary. A four bar linkage constrained to remain vertical can accomplish this. As the joints slide up or down relative to each other, they move closer together, and the vertical supporting bars move closer as well. The connection to the motors should not change, so the motors should also move with the joints by mounting them on a four bar linkage with the same horizontal distance apart.

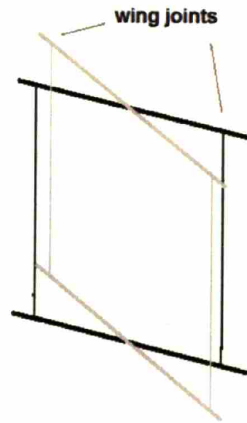


Figure 21: Diagram of changing the stroke plane by changing the heights of the wing joints. A four bar linkage keeps the vertical bars upright while the joints rotate about a fixed point.

Figure 22 shows the Solidworks model of the prototype. A middle bar constrained to remain vertical keeps the vertical supports vertical as the stroke plane changes. Cables form two bars of a four bar linkage with the two joints and a lever arm that controls the angle of the stroke plane. As the horizontal distance between the joints shortens, the horizontal distance between the cables also shortens, so that there is no need to account for changing vertical cable lengths due to angled cables.

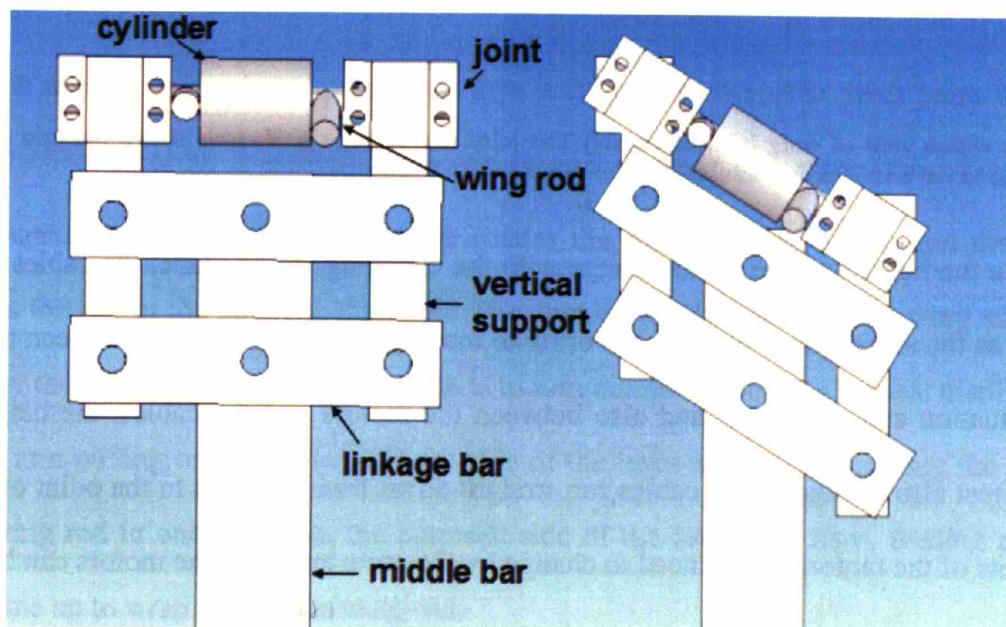


Figure 22: (Front view of wing joint assembly) Solidworks model illustrating changing stroke plane.

The first design included only a hollow cylinder surrounding the two ends of the wing rods that caused the wing rod to rotate with the changing heights of the joints. However, the cylinder overlapped with only a short section of the rod, creating a situation where the rod could catch on the cylinder as it rotated. An additional bar was added to cause rotation in the joints rather than the rods (Figure 23). The cylinder is no longer necessary, but has been retained to provide additional stability.

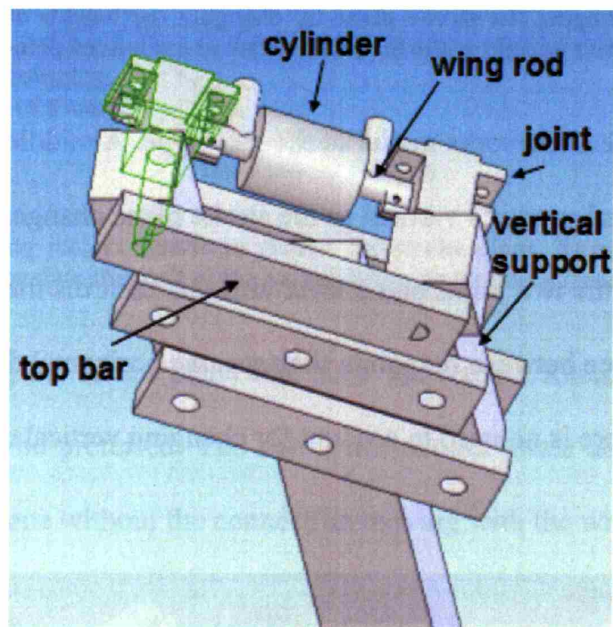


Figure 23: (Back view of wing joint assembly) The joint end forms a half circle which fits into a hole of the same shape in the bar. The bar causes the two joints to rotate together.

Since the heights of the joints change with the changing stroke plane, the cables need to be adjusted as the stroke plane changes. In order to maintain the same relation between the point of cable actuation and the joints, and also between the motors and the cables, the heights of the motors must also change. If the cables run straight down from the joint to the point of actuation, the heights of the motors would need to change by the same amount. The motors can be mounted

on another four bar linkage that would create the same relative vertical and horizontal motions as those in the joints (Figure 24).

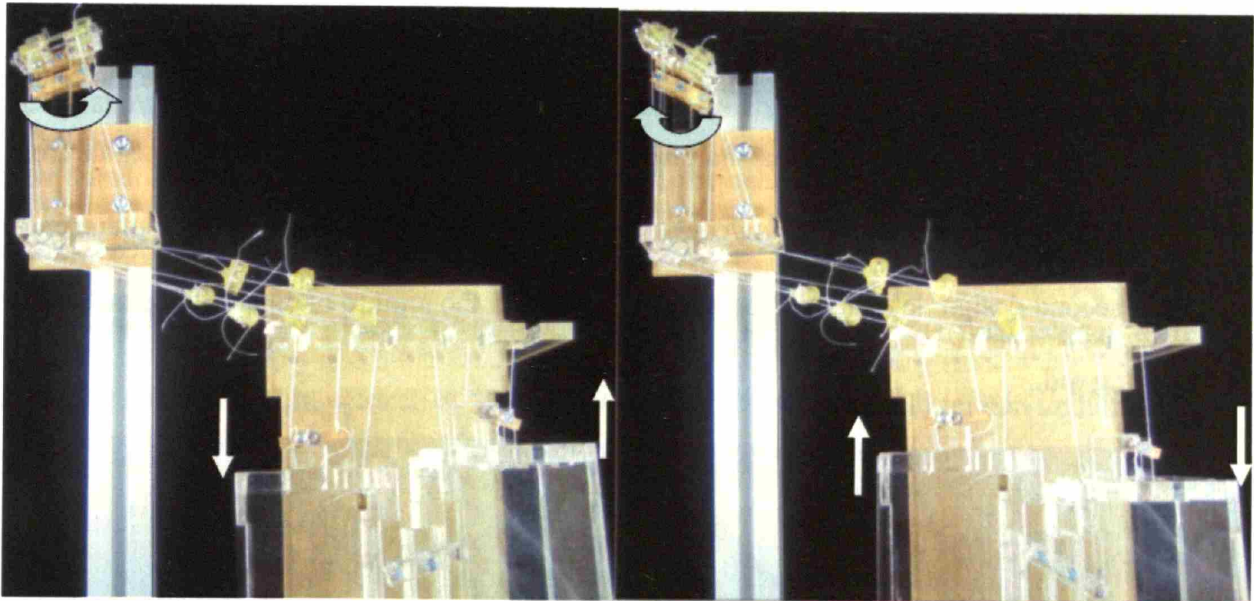


Figure 24: As the motor cases move up and down, the stroke plane of the wing also changes, keeping the relationship between the motor and wing joint the same throughout changing stroke planes. Both the motor units and the wing joints use a four bar linkage to change height

4.2.2 Flapping actuation

In the previous cable design for the direct drive, the cables pulled on either side of the pivot point of each wing support. A minor concern here was how far from the pivot point the cable could be attached. In order to address this concern and also use less space, the wing support could be rotated instead of pulled. One cable rotates the rod in one direction, and the second cable rotates the rod in the opposite direction. The angular displacement of the wing support is controlled by the length of string pulled, which is in turn determined by the vertical displacement of the lever arm pulling on the cables. As one side of the lever arm lowers, pulling the cable to rotate the wing rod in one direction, the opposite side of the lever arm rises, feeding an equal length of cable up to wrap around the wing rod.

Since the cables are now being pulled directly below the joint, the cable will not be tangent to the cross section of the wing rod. The length of cable wrapped around the rod will change slightly with changing stroke plane. In order to prevent this, the cable can be directed horizontally through a guide before being directed down to the actuating lever. The initial design, shown in Figure 25 labeled '1', used a pulley on the vertical support to guide the cable from the wing rod down below the joint. However, new angles are introduced as the stroke plane changes. In the second design, labeled '2', the guides rotate with the joint to maintain the same angle with the wing rod.

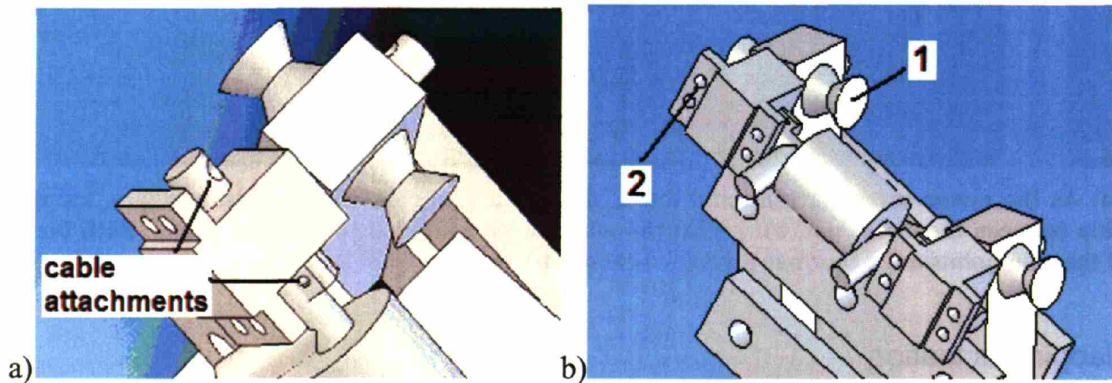


Figure 25(a): Solidworks model showing the cable attachment points on the wing rod. One cable goes through each attachment point to rotate the wing rod in each direction. (b) Solidworks model showing the first and second methods for guiding the cable down (cable attachment points hidden, please refer to figure a). In the first method, labeled 1, the pulley is on the vertical support, and as the stroke angle changes, the relationship between the wing rod and the pulley changes. In the second method, labeled 2, the guides for the cable are on the joint, which rotate along with the wing rod.

The vertical displacement of the lever arm-cable connection point should equal the length of string wrapping around the wing rod. In order to achieve this, the section of cable connecting to the lever arm must run in the same direction as the displacement of the lever arm, and the cable connecting to the wing rod should be directed perpendicularly away from the rod.

4.2.3 Cable guides

Since the motor diameter is larger than the footprint of the thorax, the cables need to be guided away from underneath the thorax where the wing structures are. The layout of the motor casings is shown in Figure 26. The cables should run down close to the body of the wing structure stand. About 70 mm underneath the wing rods, the cables turn to run horizontally to the motors. Since the 70 mm is approximately equal to the length of the wing and the wing is angled forward, there is more than enough clearance for the wing to flap. For the final design, there should be consideration of how much of the air surrounding the wing should remain undisturbed, and the height, or the distance between the wing rod and the widening of the base, should be increased accordingly.

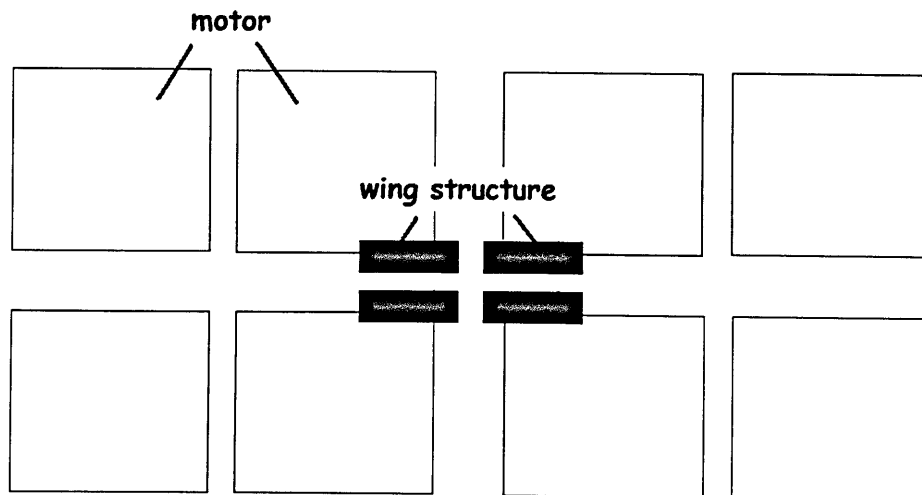


Figure 26: Overhead view of the layout of the four flapping mechanisms for each of the four wings, and the eight motors required to drive the mechanisms (two motors per wing)

The first design for guiding the cables included grooved ‘pulleys’ at the bottom of the wing structure stand. However, it is much simpler to have holes with an additional curved bearing surface rather than pulleys mounted at an angle. The cables run horizontally from the bottom of

the stand to above the motors. Another pulley turns the cable to run vertically down to the connection to the lever arm. The schematic is shown in Figure 27. The Solidworks model of the guides that turn the cables out to the motors is shown in Figure 28. The actual bearings of the prototype are shown in Figures 29 and 30.

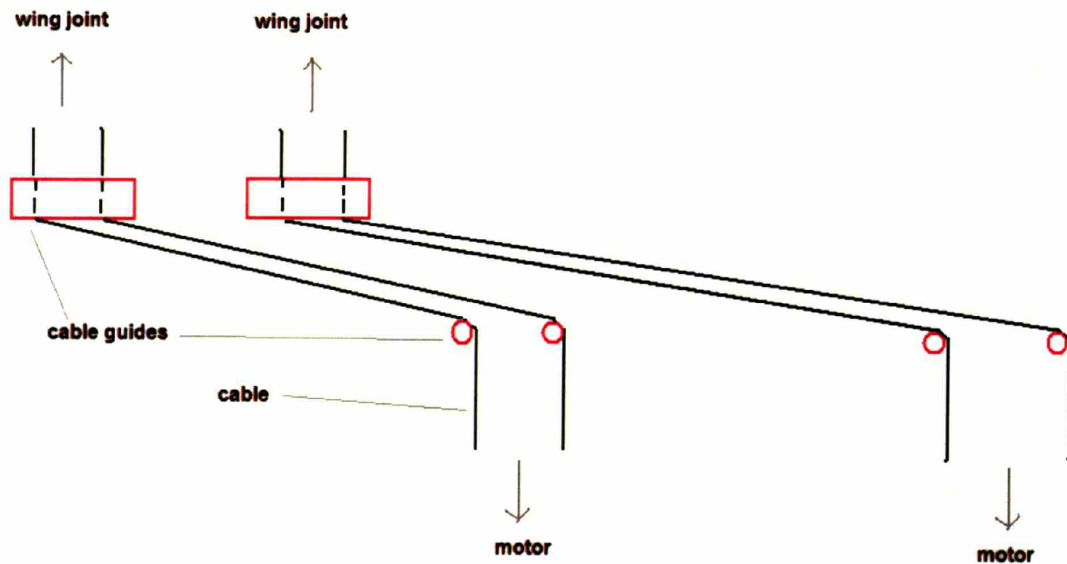


Figure 27: Schematic of cable system. The cables run vertically down from the wing joint, through a guide that turns the cables to run horizontally to another guide that turns the cables to attach vertically to the lever on the motor.

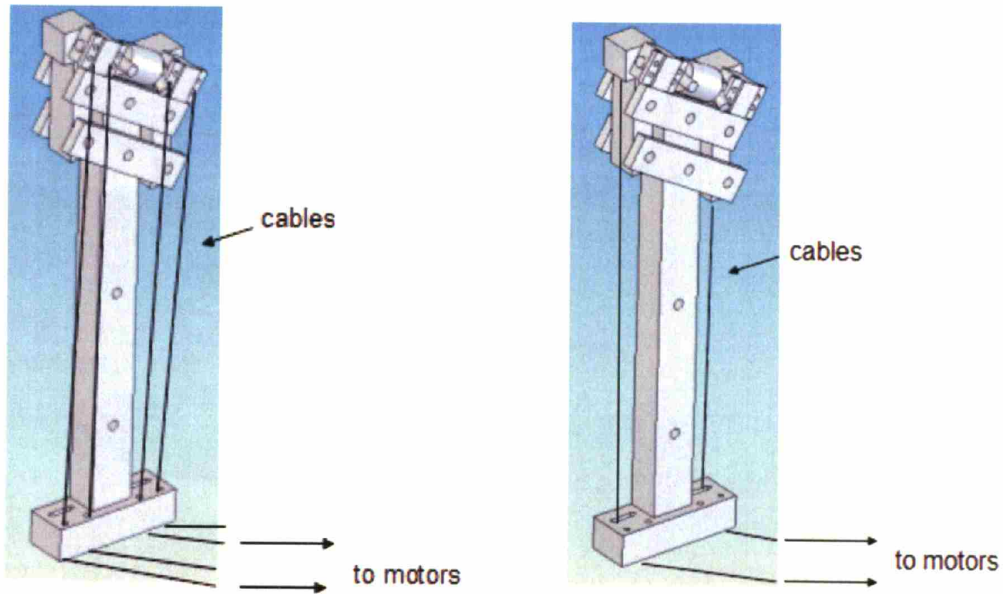


Figure 28: Cables that actuate the flapping motion run down from the joint through the four circular holes in the front (left). Cables that change the stroke plane run from the vertical supporting bar down through the slots (right).

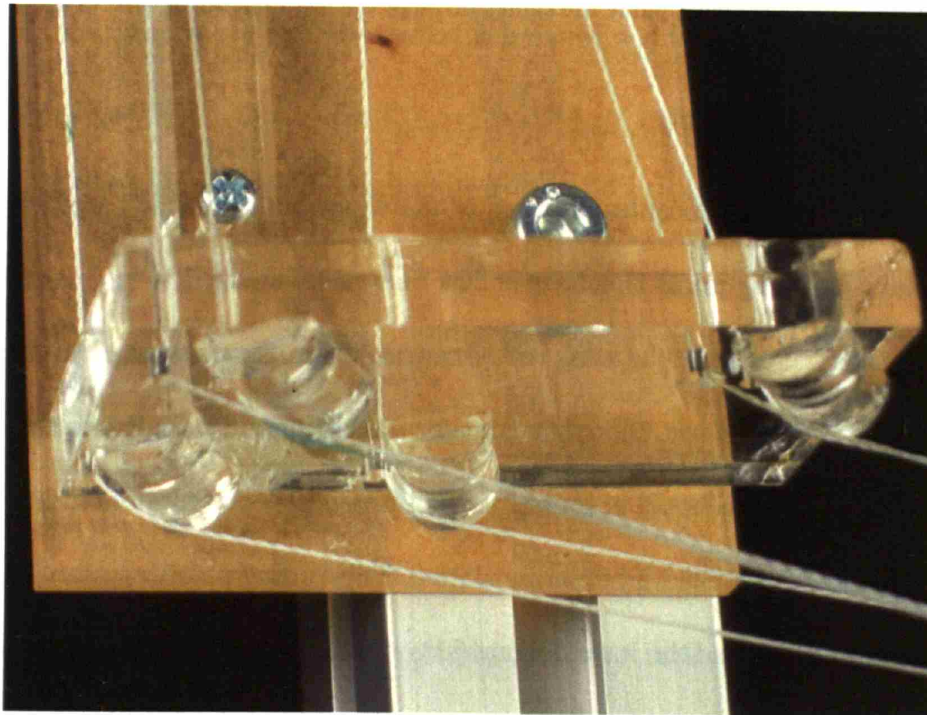


Figure 29: Round bearing surface below the wing unit to guide the cables through a sharp turn



Figure 30: Rounded bearing surfaces guide the cables through the last turn downward to the actuating lever arm

4.2.4 Motor and lever assembly

The lever arms driving the cables attached to the wing rods sit in the base several hundred millimeters below the wing joints. Each lever has one cable attached to each end to drive the back and forth rotating motion of the wing rod. One end of the lever is driven by a linear actuator that will push and pull on the arm. Since the actuator travels in a linear path and the lever travels in an arcing path, the interface must account for the different types of motion. Either the actuator connection can pivot, or the lever arm can be slotted. This prototype uses a slot as the interface between the motor actuator and the lever (Figure 31).

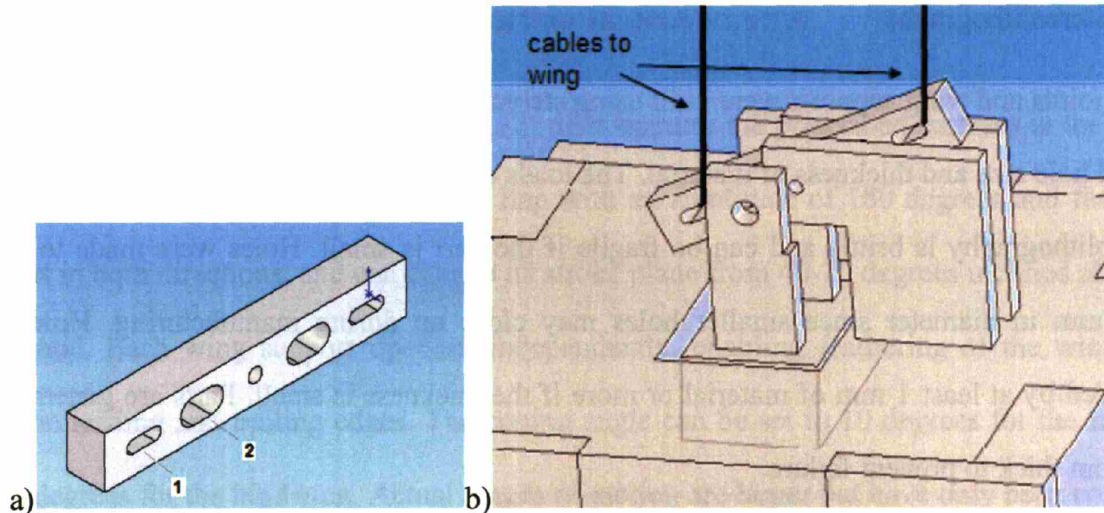


Figure 31(a): The lever arm contains slots for the cables and actuator. The cable attaches to the slot labeled 1. The actuator will be connected with the slot labeled 2. **(b):** The lever arm sits on top of the motor casing. The actuator will push on the block shown in light gray lines, which will transfer the force to the lever arm.

The BioInstrumentation Lab has custom-built Lorentz force linear actuators available that can give displacements of 2-4 mm at 40 Hz with an output of a few Newtons. Each motor is roughly 40 mm in diameter and 100 mm tall. Each motor sits in a separate case, with the lever unit and cable guide on top.

4.2.5 Prototype dimensions and manufacturing

The prototype was designed for a wing and thorax that were scaled by a factor of four. Specifically, the wing supports are 12 mm apart rather than 3 mm, and the distance between two wings is 32 mm, rather than 8 mm. Each wing joint assembly has a footprint of about 25 by 14 mm. Each dimension in the prototype is not necessarily four times as large as a mechanism that is to scale, since many of the dimensions were chosen based on the limitations of manufacturing with the tools available for use. Stereolithography and laser cutting were used in addition to a mill to build the prototype.

4.2.5.1 Stereolithography

The joints and wing supports were built using stereolithography. The limitations in the design included hole size and thickness of material. The loads on the parts are low, but the material used in stereolithography is brittle and can be fragile if the part is small. Holes were made to be at least 1 mm in diameter since smaller holes may close up during manufacturing. Holes are surrounded by at least 1 mm of material or more if the thickness is small. Parts are generally at least 2 mm thick to prevent failure.

4.2.5.2 Laser Cutting

The laser cutter was used to cut acrylic to make the supporting structures and linkages, which were generally rectangular. One issue in using the laser cutter is the taper of the cut. With the 2 mm and 3 mm acrylic, the taper was not as obvious and the parts fit easily with little modification. With the 6 mm acrylic, small holes needed to be remachined using a drill press. To create more accurate fits, smaller pilot holes were made with the laser cutter, and then bigger holes were drilled. Because of the taper, very small holes cannot be made with the laser cutter with great precision.

4.2.6 Mounting and setting the coning angle

In setting the coning angle, all components of the flapping mechanism must rotate together in order to keep the relationships of the cables constant. In this prototype, MK positioning bars were used to hold the components up. The pivot point lies directly below the midpoint between the two wing joints. There is some space remaining between the fore and hind wing setups to allow for the coning angle to change. Future designs can place the two setups closer together if the bases are cut so that there is no collision when the coning angles increase.

5. Evaluation of the prototype and further improvements

The prototype built (shown in Figure 32) demonstrates the prescribed motions at the base of a dragonfly wing. It can cause a wing to flap with an amplitude of 180 degrees and feather 60 degrees in both directions, and can change its stroke plane from 40-70 degrees inclined above the horizontal. Each wing support operates independently, enabling feathering of the wing about both the leading and trailing edges. The coning angle can be set to 10 degrees for the forewing and 2 degrees for the hindwing. Actual ranges of motion are larger but have only been confirmed for the ranges specified in the performance criteria.

The prototype is scaled to four times the size of the final device and cannot be operated at 40 Hz as it is meant only to illustrate the kinematics of the wing. Further iterations should use different methods of manufacturing and fit within a roughly 10 mm wide thorax casing. This prototype only contains two wings—a forewing and a hindwing on the same side of the body. Mounting methods result in dimensions that are much larger than the design constraints specify.

In changing the stroke plane, cables that pull on the vertical supporting bars do not remain vertical as the stroke plane changes. There are slight angle changes as the stroke plane varies, so the change in stroke plane produced at the base does not translate perfectly at the wing unit.

It was at first difficult to flap the wing supports in the prototype. Since the joints and wing rods were made with stereolithography, there was a significant amount of friction due to a tight fit and rough surfaces. The bearing surface for the rods was not long enough—the cylinder in the center was not stable enough to act as a bearing as it was not fixed to either joint. There was also a lot of friction between the cable and the cable guide in the joint as the joint was too small to add a bearing surface to. To address these issues, lubricant was added to the wing rod-joint interface. The middle cylinder was removed and a thin rod was added through the center of both

wing rods, creating a long bearing surface for both wing rods. A bearing surface for the cables below the joint was also added and attached to the four-bar linkage (Figure 32). However, this bearing extends past where the thorax casing should end. In future iterations, the cables should be directed towards the inside of the thorax rather than away from it since there is more space to add a bearing surface on the inside of the wing pivot point (Figure 33). Lengthening the joint in which the wing rod rotates will also provide a better bearing surface and may eliminate the need for a pin through the wing rods.

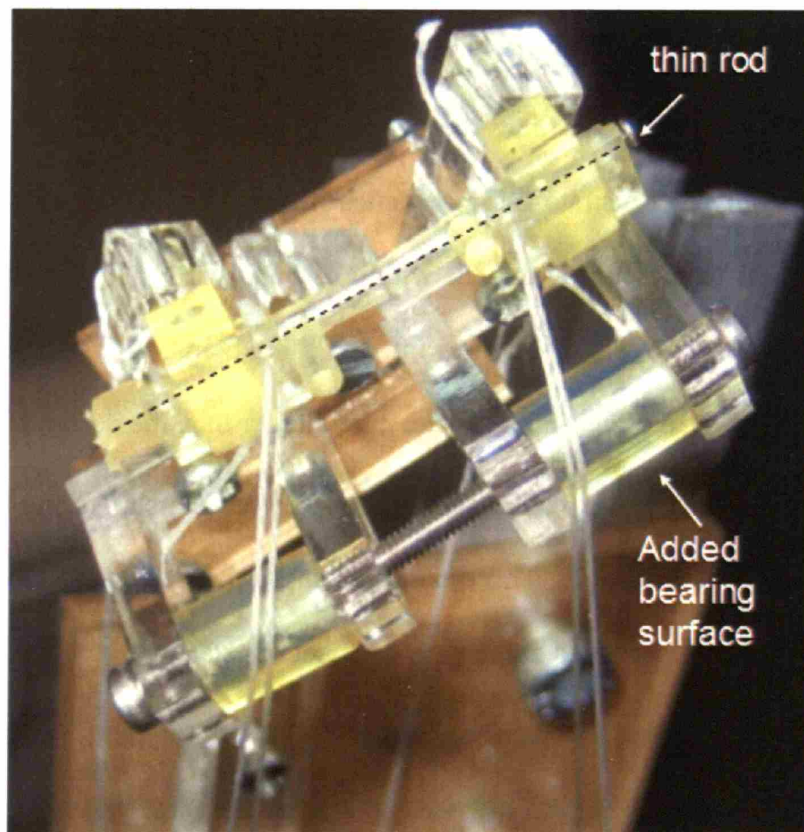


Figure 32: A thin rod was inserted through both wing rods, acting as a bearing for the rotation of the wing rods. A bearing surface was also added for the cables extending from the joint.

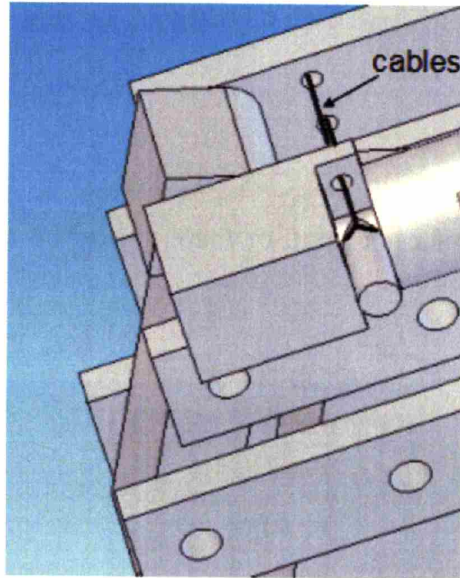


Figure 33: In the new design, cables attach to the wing rod and are directed away from the wing towards the thorax. A bearing surface is added to the back of the bar (not shown).

The cables go through a few right angle turns from the wing rod to the lever arm. For each turn, there should be a bearing surface to reduce friction between the cable and guide. The resulting velocity of the cables is about 100-200 mm/s depending on the diameter of the wing rod. If the material that the cable runs through is soft, even minimal wear can cause a significant change in the part. More importantly, if there is high friction between the cable and the cable guides, the amount of force required to pull the same load is increased. With three approximately right angle turns, the force required would increase dramatically without bearing surfaces, making it difficult to actuate the wing supports. The prototype uses curved acrylic pieces to act as bearing surfaces since they were easy to attach to the existing acrylic pieces. For the final design, a smoother surface should be used.

In the existing prototype, the two cables for each wing joint were placed too close together. Since the thin rod was placed through the wing rod, the second attachment point could no longer be used since the hole was filled by the rod. Figure 34 shows the original attachment points for

the two cables. The second cable was then attached to the same point as the first cable, causing the exit points to be close together. As seen in Figure 35, the cables interfere with each other as a result of the two cables exiting the joint on the same side. In the final design, the cables should be placed on opposite sides of each joint, or there should be additional guides to separate the cables.

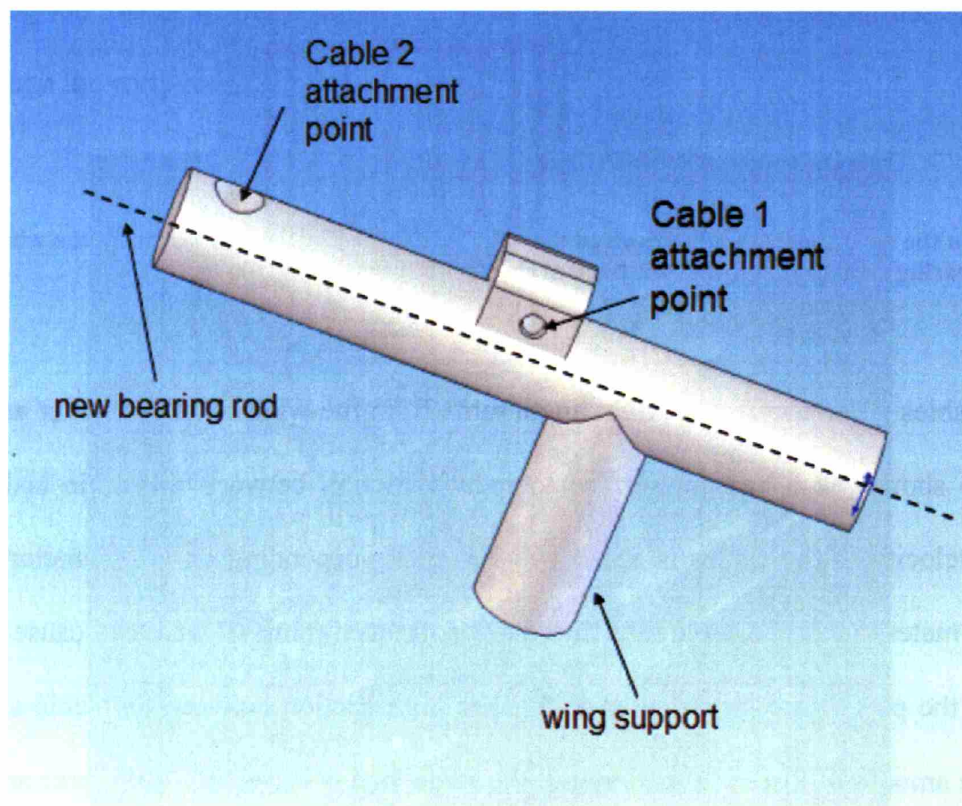


Figure 34: Original cable attachment points on the wing rod

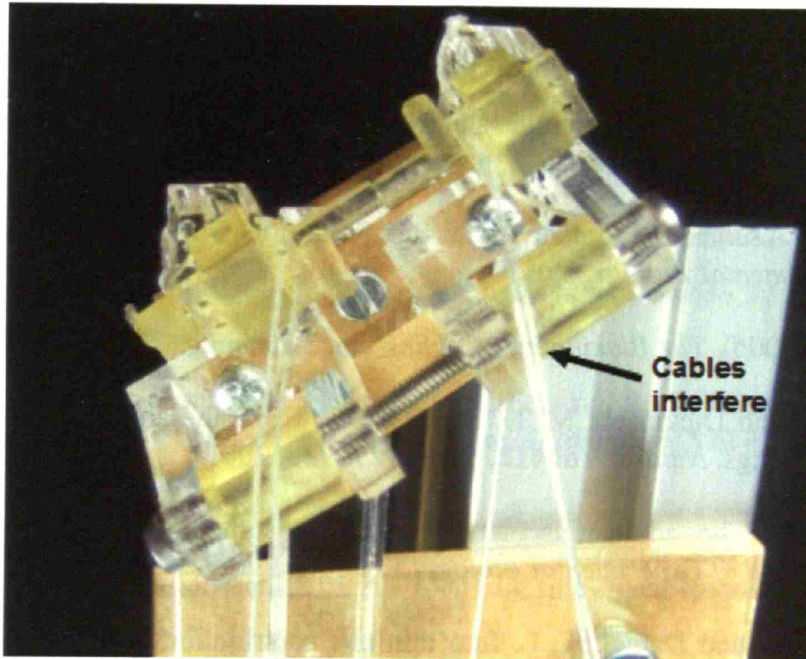


Figure 35: Since the two cables are close together, the cables sometimes interfere with each other.

In the higher joint, the cables also interfere with the wing support due to the added bearing surface. By directing the cables behind the wing joint assembly, this issue will no longer be a problem.

Fasteners were not accounted for in the design of the flapping mechanism. In the actual mechanism, the bolts protrude further than is ideal, interfering with the path of the cables. New fasteners can be chosen that do not extend as far.

In future iterations of the flapping mechanism, special attention should be paid to the bearing surfaces in order to reduce friction and minimize the forces required to actuate the wing. The wing will be flapping at 40 Hz, so it is important that all rotating parts can slide smoothly against their respective surfaces. Some additional design work needs to be done in order to fit all four wing units into the specified thorax size constraint. Adjustments to the angles of the cables and more precise tensioners are needed in order to keep the tension consistent as the stroke plane changes.

References

- Alexander, D. E. Wind tunnel studies of turns by flying dragonflies. *Journal of Experimental Biology*. Vol 122, issue 1, pages 81-98, 1986.
- Azuma, A., Azuma, S., Watanabe, I., and Furuta, T. Flight mechanics of a dragonfly. . *Journal of Experimental Biology*. Vol 116, pages 79-107, 1985.
- Azuma, A. (2006). *The Biokinetics of Flying and Swimming*, 2nd Ed. AIAA Inc.
- Birch, J. M. and Dickinson, M. H. Spanwise flow and the attachment of the leading-edge vortex on insect wings. *Nature*. Vol 412, pages 729 -733, 2001.
- Clark, H. W. The adult musculature of the anisopterous dragonfly thorax (Odonata, Anisoptera). *Journal of Experimental Biology*. Vol 67, pages 523-526, 1940.
- Combes, S. A. and Daniel, T. L. Into thin air: contributions of aerodynamic and inertial-elastic forces to wing bending in the hawkmoth *Manduca sexta*. *Journal of Experimental Biology*. Vol 206, pages 2999-3006, 2003.
- Dickinson, M. H., Lehmann, F-O., and Sane, S. P. Wing rotation and the aerodynamic basis of insect flight. *Science* Vol 284, pages 1954 -1960, 1999.
- Ellington, C. P., Van den Berg, C., Willmott, A. P., and Thomas, A. L. R. Leading-edge vortices in insect flight. *Nature* Vol 384, pages 626-630, 1996.
- Neville, A. C. Aspects of flight mechanics in Anisopterous dragonflies. *Journal of Experimental Biology*. Vol 37, 631-656, 1960.
- Ruppell, G. Kinematic Analysis of symmetrical flight manoeuvres of Odonata. *Journal of Experimental Biology*. Vol 144, pages 13-42, 1989.
- Sane, S. P. The aerodynamics of insect flight. *Journal of Experimental Biology*. Vol 206, pages 4191-4208, 2003.
- Simmons, P. J. The neural control of dragonfly flight. I. Anatomy. *Journal of Experimental Biology*. Vol 71, pages 123-140, 1977.
- Van Den Berg, C.. and Ellington, C. P. The vortex wake of a 'hovering' model hawkmoth. *Philosophical Transactions of the Royal Society of London, series B*. Vol 352, no. 1351, pages 317-328, 1997.
- Wakeling, J. M. and Ellington, C. P. Dragonfly flight (2). Velocities, accelerations and kinematics of flapping flight. *Journal of Experimental Biology*. Vol 200, pages 583 -600, 1997.

Wang, H., Zeng, L. J., Liu, H. and Yin, C. Y. Measuring wing kinematics, flight trajectory and body attitude during forward flight and turning maneuvers in dragonflies. *Journal of Experimental Biology*. Vol 206, pages 745 -757, 2003.

Wang, Z. J. Dissecting insect flight. *Annual Review of Fluid Mechanics*. Vol 37, pages 183-210, 2005.

Wootton, R. J. Functional morphology of insect wings. *Annual Review of Entomology*, Vol 37, pages 113-140, 1992.

Yan, J, Wood, R. J., Avadhanula, S. , Sitti, M., and Fearing, R. S. Towards flapping wing control for a Micromechanical Flying Insect. *Robotics and Automation*, Vol 4, pages 3901-3908, 2001.

Yan, J. and R.S. Fearing. Wing Forces Map Characterization and Simulation for the MicroMechanical Flying Robotic Insect, IEEE Int. Conf. on Intelligent Robots and Systems, Oct 28-30, 2003, Las Vegas NV.

Zbikowski, R., Galinski, C., and Pederson, C. A four-bar linkage mechanism for insect-like flapping wings in hover: Concept and an outline of its realization. *Journal of Mechanical Design*, Vol 127, Issue 4, pages 817-824, 2005.

Appendix A

Calculation of torque required of wing

Total torque = torque due to drag + torque due to inertia (small)

Torque due to drag:

$$\tau = \frac{1}{2} \rho \omega^2 C_d W \frac{1}{3} L^3$$

where $\rho = 1.293 \text{ kg/m}^3$, $C_d = 1.17$, $W = 15 \text{ mm}$, $L = 70 \text{ mm}$

ω was estimated from linear stroke velocities of wings documented by Ruppell (1989)

	wing length (mm)	wingbeat frequency (Hz)	max stroke velocity (mm/s)	max angular velocity (rad/s)	torque (Nm)
insect					
A.c.	45.1	36	2920	129.490	5.430E-03
An.i. (hindwing)	47.5	37	2070	87.158	2.874E-03
An.j. (male)	51	36	2940	115.294	6.224E-03

Abbreviations used for Anisoptera Aeshnidae:

A.c.: *Aeshna cyanea*

An.i.: *Anax imperator*

An.j.: *Anax junius*

Notes:

Calculations are only estimates since the data are not necessarily correlated across the table, as the data are taken from separate tables.

Linear stroke velocity is reported for half the wing length.

Maximum angular velocity = maximum stroke velocity/(wing length/2)

6707-61